



International Journal of Control Theory and Applications

ISSN : 0974-5572

© International Science Press

Volume 9 • Number 43 • 2016

Discrete Lagrangian Mathematical Model Based Sensorless Two DOF Control of Induction Motor

Manoj Swargiary^a, Jayati Dey^b and Tapas Kumar Saha^c

^{a-c}Department of Electrical Engineering, National Institute of Technology Durgapur-713209, India. Email: ^amanoj_sargu@gmail.com; ^bdeybiswasjayati@gmail.com; ^ctapassahanit@gmail.com

Abstract: This paper addresses development of sensor less control strategy for induction motor (IM) drives. The control strategy is developed based on the derived discrete time synchronous frame IM model through the formulation of discrete lagrangian. The control scheme mimics the conventional continuous time vector control. The control strategy utilizes the robust compensation and loop shaping property of discrete time two degree of freedom (DOF) control to ensure satisfactory gain and phase margins. The controllers are designed through root locus technique. Further, a discrete time model reference adaptive system (MRAS) observer is derived for the speed sensor less control of the IM drive for the discrete IM dynamics. The performance of the two DOF control strategy is compared with discrete PI control. The effectiveness of the controller is also found out successfully with MRAS observer even in presence of high load disturbance.

Keywords: Induction Motor Drives, Discrete Time Modelling, Discrete Two Degree of Freedom, Discrete MRAS, Vector Control.

1. INTRODUCTION

As an effort of designing discrete-time controllers for IMs based on sampled models, one can find some control approaches based on the classical explicit Euler approximation as in [2]-[4]. However, this sometime represents the continuous time system dynamics badly in discrete domain. That may lead to wrong controller parameter design [1]. Instead, [1] proposes discrete time modelling of the IM with the help of geometric integration technique, variational integration in stationary two-phase $\alpha - \beta$ frame. In this work, the proposed stationary frame model is transformed into the synchronously rotating d-q frame model. Afterward conventional like rotor field orientation control strategy is derived and implemented for discrete time d-q frame IM dynamics.

Degree of freedom of a control system is the number of closed loop TFs that can be adjusted to achieve the predefined goals [10]. As controller design process is multi objective process, to fulfil each objective with one degree of freedom may not be suitable [10] and hence the two DOF control. Different two DOF PID control strategies are mentioned in [6]-[10]. However, it is noticed that, in the IM application

of two DOF control the two DOF control strategy is applied to only the inner current control loop or outer speed control loop at a time. In this work, the root locus design technique for two DOF strategy is utilized and two DOF controller is designed for all the inner loops (d-axis component of stator current and q-axis component of stator current) and outer loops (speed and flux) to achieve good set point tracking and load disturbance rejection. The performances are also compared with a discrete PI controller designed with same bandwidth.

Further, through the last few decades, there has been a significant rise of interest in sensor less induction motor drives without mechanical speed sensors. Such drives are attractive because of their low cost and high reliability, also it is free from maintenance cost of mechanical sensor. Different speed estimation techniques are described in [11]-[17], where the fundamental machine model is utilized to design model reference adaptive systems (MRAS), nonlinear observers, extended Kalman filters, or adaptive observers. In this work a discrete time MRAS observer is adopted which is based on the derived discrete IM dynamics.

This work achieves the following objectives for IM drives.

- Using root locus and loop shaping technique, development of a control strategy for derived discrete time induction motor dynamic modal that replicates the conventional vector control strategy of continuous time induction motor drives.
- Design and analysis of robustness and performance of two DOF controller. The performance of two DOF control is compared against that of a discrete PI control.
- Derivation of a discrete MRAS observer in context with the discrete IM dynamic model for sensor less operation of adjustable IM speed drive.

2. DISCRETE TIME MODEL OF INDUCTION MOTOR

The stationary ($\alpha - \beta$) frame IM dynamics for IM derived through the formulation of discrete lagrangian can be written as (1) [1], [5].

$$\begin{aligned} \omega_{k+1} &= \omega_k - \frac{f_v}{J} h \omega_k + \mu_d h I_{\alpha\beta sk}^T \Gamma \phi_{\alpha\beta rk} - \frac{h}{J} \tau_{Lk} \\ \phi_{\alpha\beta rk+1} &= \alpha_d e^{\Gamma h p \omega_k} \phi_{\alpha\beta rk} + L_m \alpha \alpha_d h e^{\Gamma h p \omega_k} I_{\alpha\beta sk} \\ I_{\alpha\beta sk+1} &= \gamma_d I_{\alpha\beta sk} + \beta_d \alpha_d \phi_{\alpha\beta rk} - \beta_d \alpha_d^2 e^{\Gamma h p \omega_k} (\phi_{\alpha\beta rk} + L_m \alpha h I_{\alpha\beta sk}) + \frac{h}{\sigma_d} U_{\alpha\beta sk} \\ \phi_{\alpha\beta sk+1} &= \phi_{\alpha\beta sk} - h R_s I_{\alpha\beta sk} + h U_{\alpha\beta sk} \end{aligned} \quad (1)$$

where, p = pole pair; ω_k = angular speed; J = moment of inertia; f_v = friction coefficient; h = sampling time; $I_{\alpha\beta sk}$ = stator $\alpha - \beta$ component of stator current components; $\phi_{\alpha\beta rk}$ = rotor $\alpha - \beta$ component of stator current components; $\alpha = R_r/L_r$; $\alpha_d = 1/(1 + h\alpha)$; $\mu_d = \mu\alpha_d$; $\mu = 3L_m p/2JL_r$; $\sigma = L_s - L_m^2/L_r$; $\sigma_d = \sigma + \alpha\alpha_d h L_m^2/L_r$; $\beta_d = L_m/\sigma_d L_r$; $\gamma_d = 1 - R_s h/\sigma_d$; $\Gamma = \begin{bmatrix} 0 & -1 \\ 1 & 0 \end{bmatrix}$; $e^{\Gamma\theta} = \begin{bmatrix} \cos \theta & -\sin \theta \\ \sin \theta & \cos \theta \end{bmatrix}$.

Now to obtain synchronous ($d - q$) frame model from the stationary ($\alpha - \beta$) frame model the d axis is aligned with the rotor flux axis [17], [18] as shown Figure 1(a). Hence the $d - q$ discrete IM model frame is given by

$$\omega_{k+1} = \omega_k - \frac{f_v}{J} h \omega_k + \mu_d h \left(I_{\alpha\beta sk} e^{-\Gamma h p \rho_k} \right)^T \Gamma \left(\phi_{\alpha\beta rk} e^{-\Gamma h p \rho_k} \right) - \frac{h}{J} \tau_{Lk}$$

$$\phi_{\alpha\beta rk+1} e^{-\Gamma h p \rho_{k+1}} = \left(\alpha_d e^{\Gamma h p \omega_k} \phi_{\alpha\beta rk} + L_m \alpha \alpha_d h e^{\Gamma h p \omega_k} I_{\alpha\beta sk} \right) e^{-\Gamma h p \rho_{k+1}} \quad (2)$$

$$I_{\alpha\beta sk+1} e^{-\Gamma h p \rho_{k+1}} = \left(\gamma_d I_{\alpha\beta sk} + \beta_d \alpha_d \phi_{\alpha\beta rk} - \beta_d \alpha_d^2 e^{\Gamma h p \omega_k} (\phi_{\alpha\beta rk} + L_m \alpha h I_{\alpha\beta sk}) + \frac{h}{\sigma_d} U_{\alpha\beta sk} \right) e^{-\Gamma h p \rho_{k+1}}$$

$$\phi_{\alpha\beta sk+1} e^{-\Gamma h p \rho_{k+1}} = \left(\phi_{\alpha\beta sk} - h R_s I_{\alpha\beta sk} + h U_{\alpha\beta sk} \right) e^{-\Gamma h p \rho_{k+1}}$$

Now considering $\omega_s = (\rho_{k+1} - \rho_k)/h$ as sampled version of synchronous speed and I_{dqsk} as $d-q$ component of stator current, the discrete IM dynamic model is obtained as (3)

$$\omega_{k+1} = \omega_k - \frac{f_v}{J} h \omega_k + \mu_d h I_{dqsk}^T \Gamma \phi_{dqrk} - \frac{h}{J} \tau_{Lk}$$

$$\phi_{dqrk+1} = \alpha_d e^{-\Gamma h p (\omega_s - \omega_k)} \phi_{dqrk} + L_m \alpha \alpha_d h e^{-\Gamma h p (\omega_s - \omega_k)} I_{dqsk}$$

$$I_{dqsk+1} = \gamma_d e^{-\Gamma h p \omega_s} I_{dqsk} + \beta_d \alpha_d e^{-\Gamma h p \omega_s} \phi_{dqrk} - \beta_d \alpha_d^2 e^{-\Gamma h p (\omega_s - \omega_k)} (\phi_{dqrk} + L_m \alpha h I_{dqsk}) + \frac{h}{\sigma_d} e^{-\Gamma h p \omega_s} U_{dqsk}$$

$$\phi_{dqsk+1} = e^{-\Gamma h p \omega_s} \phi_{dqsk} - h R_s e^{-\Gamma h p \omega_s} I_{dqsk} + h e^{-\Gamma h p \omega_s} U_{dqsk}$$

Block diagram of the discrete synchronous frame IM is shown in Figure 1(b).

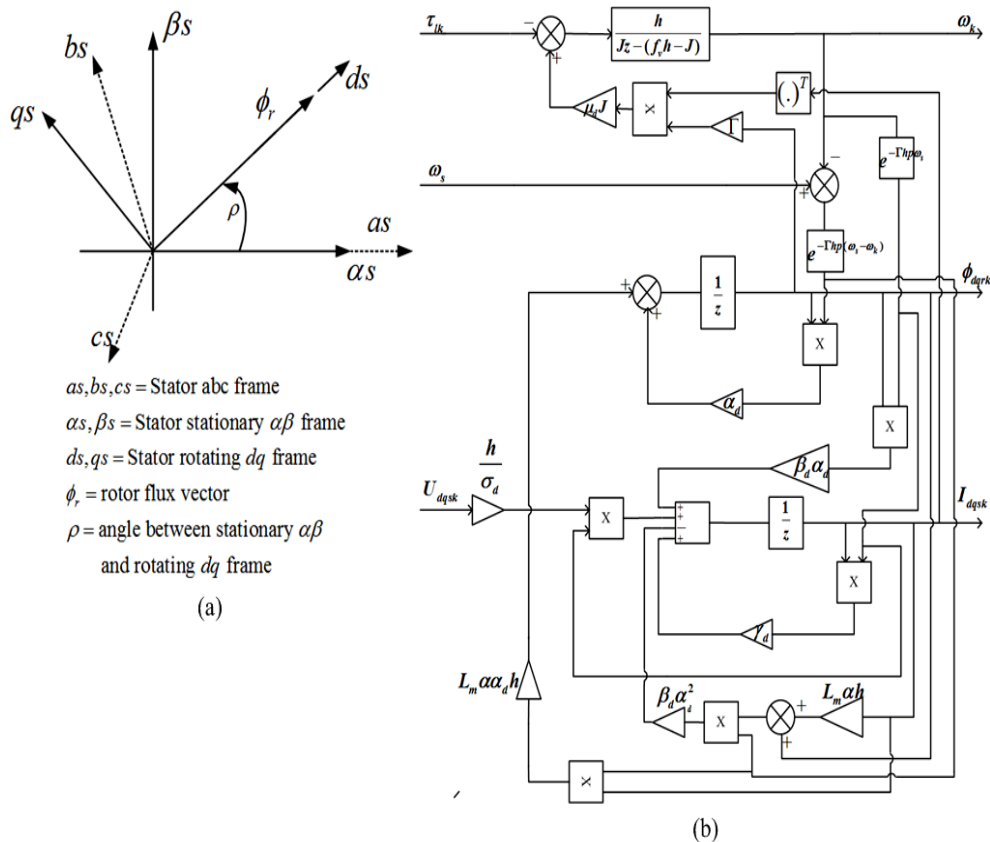


Figure 1: (a) Vector representation of reference frame, (b) Block diagram of the discrete IM model.

3. CONTROL STRATEGY AND TWO DOF CONTROLLER DESIGN

A. Control Strategy

In this section a control strategy is developed for the discrete IM model that, replicates the conventional continuous time control of IM drives. The IM model (3) is associated with trigonometric terms $e^{-\Gamma hp\omega_s}$ and $e^{-\Gamma hp(\omega_s - \omega_k)}$. These terms are removed through small-angle approximation, since $hp\omega_s$ and $hp(\omega_s - \omega_k)$ are very small (in this case 0.0001 sec). The small angle approximation is required to decouple the d and q axis components.

Considering the field orientation is perfect i.e., $\phi_{qrk} = 0$ together with the small angle approximation a relation between ϕ_{drk} and I_{dsk} can be obtained from the d component of the rotor flux equation in (3) as (4)

$$\phi_{drk} / I_{dsk} = L_m \alpha \alpha_d h / (z - \alpha_d) \quad (4)$$

Thus from the measured d axis component of stator current, the d axis flux component can be estimated from (4) and thus ϕ_{drk} becomes $\hat{\phi}_{drk}$. The slip speed can be estimated from (5) with measurable q axis component of stator current. Which will be utilized in indirect field orientation control just like the conventional continuous time control.

The slip speed is written from the q -flux equation as (5).

$$\omega_{slip} = L_m \alpha I_{qsk} / p \hat{\phi}_{drk} \quad (5)$$

Again from the stator flux equation in (3), together with the relations $\phi_{dqsk} = L_s I_{dqsk} + L_m I_{dqrk}$ and $\phi_{dqrk} = L_r I_{dqrk} + L_m I_{dqsk}$ and small angle approximation the discrete plant transfer function (TF) for the current (inner) control loop can be written as $h / L_s z - (L_s - hR_s)$. The decoupling terms are obtained as $c_d = hp\omega_s L_s \sigma I_{qsk}$ and $c_q = -hp\omega_{sk} L_s I_{dsk} - hp\omega_s \frac{L_m \phi_{drk}}{L_s}$. Similarly, the discrete plant TF for the speed (outer) control loop can

be written between electromagnetic torque and speed from the mechanical equation in (3) as $\frac{h/J}{z - (1 - (f_v h/J))}$.

From the mechanical equation electromagnetic torque can be written as $\tau_{el} = \mu_d J I_{dqsk}^T \Gamma \phi_{dqrk}$ and is with perfect field orientation $\tau_{el} = \mu_d J I_{qsk} \hat{\phi}_{drk}$. i.e., $I_{qsk} = \tau_{el} / (\mu_d J \phi_{drk})$. The control strategy with two DOF controllers is shown in Figure 2(a). Two pairs of two DOF controllers are designed as shown in the Figure 2(a). One pair is for the outer loop which will eventually generate d and q axis component current references (I_{dsk}^* and I_{qsk}^*) and another pair is for the inner loop which will ultimately generate d and q components of voltage references (U_{dsk}^* and U_{qsk}^*).

B. Controller Design

This section presents design procedure for two DOF controller speed loop as well as current loop so as to ensure speed tracking and robust compensation. The block diagram of a two DOF control system is depicted in Figure 2(b).

$C_{f_}$, $C_{b_}$ = forward path and feedback path controllers respectively.

$C_{s_}$, $C_{c_}$ = Speed and current loop controllers respectively.

The closed loop TFs (CLTFs) from Figure 2(b) are given by (6)

$$\begin{aligned} G_{yr}(z) &= C_{f_}(z)P(z) / (1 + C_{b_}(z)P(z)) \\ G_{yd}(z) &= P(z) / (1 + C_{b_}(z)P(z)) \end{aligned} \quad (6)$$

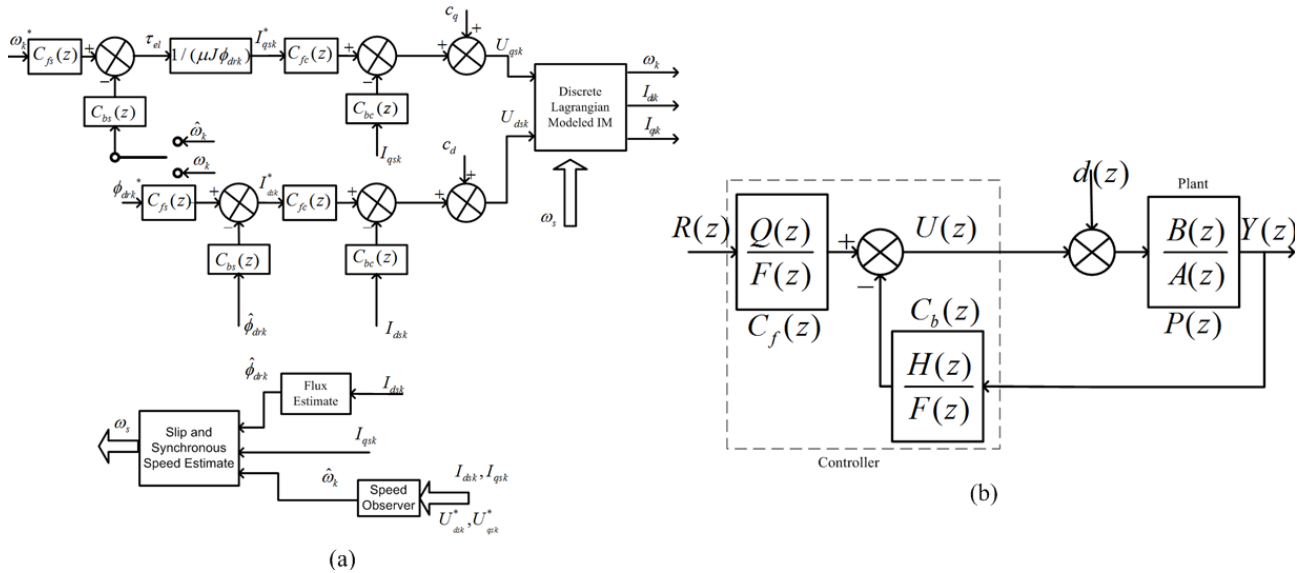


Figure 2: (a) Block diagram of the sensorless two DOF control scheme, (b) Two DOF controller structure

Thus by looking at the CLTFs it can be stated that, reference tracking is dependent on both $C_f(z)$ and $C_b(z)$ whereas disturbance response can be reformulated by adjusting the $C_b(z)$ only. These two are the responses which gives a measure of a control system performance. Thus, with two DOF control two sets of controller parameters are available to be adjusted unlike one DOF control, to achieve desired response.

The loop TF of the control structure in Figure 2(b), considering an n^{th} order plant $P(z) = B(z)/\Delta(z)$ is given by $H(z)B(z)/F(z)A(z)$. The CLTF is given by $Q(z)B(z)/\Delta(z)$ with $\Delta(z) = A(z)F(z) + B(z)H(z)$ of order $n + m$. Now the choice of m^{th} order controller polynomials $F(z)$ and $H(z)$ will characterize the pole polynomial of the closed loop system.

The design of the two DOF controller is carried out in w -plane. The CLTF of the control structure depicted in Figure 2(b) can be written in w plane as $Q(w)B(w)/\Delta(w)$ with $\Delta(w) = A(w)F(w) + B(w)H(w)$, where,

$$F(w) = w^m + f_{m-1}w^{m-1} + \dots + f_1w + f_0 \tag{7}$$

$$H(w) = k(h_mw^m + h_{m-1}w^{m-1} + \dots + h_1w + h_0) \tag{8}$$

Where, k is the gain to be obtained from the root locus.

From the controller design prospect it is to be taken into account that, the order of controller to be placed. i.e. $m + (m + 1) \geq m + n \Rightarrow m \geq n - 1$. Moreover, the desired CLTF can be defined in w -plane as $\xi B(w)/\bar{\Delta}(w)$. The constant χ is introduced to make DC gain unity. $\Delta(w)$ is the desired characteristic polynomial. After choosing $F(w)$ and $H(w)$, CLTF is obtained as $Q(w)B(w)/\Delta(w)$. However, it is prescribed to have CLTF as $\xi B(w)/\bar{\Delta}(w)$ which can be obtained by solving (9)

$$Q(w)B(w)/\Delta(w) = \xi \bar{q}(w)B(w)/\bar{\Delta}(w)\bar{q}(w) = \xi B(w)/\bar{\Delta}(w) \tag{9}$$

Where, $Q(w) = \xi \bar{q}(w)$. Thus feedback path controller gain k can be obtained by solving $\Delta(w) = A(w)F(w) + B(w)H(w) = \bar{\Delta}(w)\bar{q}(w)$. It should be pointed out that besides choice of desired closed loop pole polynomial, the choice of different $\bar{q}(w)$ provides unique solution of k .

The controllers are designed using root locus technique such that resulting loop TF $C_b(z)P(z)$ full fills the gain margin > 2 and phase margin $> 30^\circ$ to enhance disturbance rejection and robust stability.

4. DESIGN AND ROBUSTNESS ANALYSIS OF TWO DOF CONTROL SCHEME

For the verification of the proposed scheme a 1 hp IM with 4 poles 50 Hz is considered. The voltage rating of the IM is 415 Volt, stator/rotor resistances 15.12/4.24 Ω , stator, Rotor inductance/mutual inductance 0.7357H/06947 H, moment of Inertia 0.0148 Kgm^2 , mechanical damping coefficient 0.0008145 Nms, torque rating 4.91 Nm and speed rating 151.77 rad/sec.

The control scheme in Figure 2(a) is implemented in context with the controller structure shown in Figure 2(b). The design of the controller parameters are carried out with respect to the theory provided in section III.B. To ensure overall stability of the control scheme two constraints are predetermined. (i) The individual loops should be faster; and (ii) the inner loop should be faster than the outer loop. The sampling time (h) for the discrete time modelling is considered 100 μsec .

The system TF for outer loop following section III.A is obtained as $\frac{B_s(z)}{A_s(z)} = \frac{0.006757}{(z-1)}$ in z domain. The

corresponding w -plane TF can be obtained as $\frac{B_s(w)}{A_s(w)} = \frac{67.57}{(w+0.05503)}$.

Similarly, the z domain inner loop system TF is given by $\frac{B_c(z)}{A_c(z)} = \frac{0.0001}{(0.7357z-0.7342)}$ and corresponding w -plane TF is $\frac{B_c(w)}{A_c(w)} = \frac{1.359}{(w+20.55)}$.

Both outer and inner loop plants are of order one i.e. $n = 1$ and hence to fulfil the condition for controller order as mentioned in section III.B the order of the controller polynomials $F(w)$ and $H(w)$ are chosen to be $m = 1$.

1. *Controller design for speed loop:* Since the plant is of first order the corresponding root locus would be the entire negative real axis beyond the open loop pole -0.05503 in the w -plane. Hence the desired closed loop pole location is chosen at -10 so as to ensure first order overdamped response with settling time less than 1 sec. The corresponding desired CLTF is $0.148 \frac{67.57}{(w+10)}$ with $\xi = 0.148$ to make DC gain unity.

In $F(w)$ polynomial, coefficients f_1 and f_0 are set to one and zero respectively. Thus the denominator polynomial $F(w)$ becomes $F(w) = w$ i.e. $F(w)$ will provide integral action and will ensure steady state error zero.

Besides, a zero is placed to the left of the system pole to have desired loop characteristics with suitable bandwidth and phase margin. The zero is placed at -7 . Thus $H(w)$ becomes $k(w+7)$. The zero polynomial of the feed forward path compensator $q(w)$ is considered to be $(w+100)$. The gain of $H(w)$ polynomial k is obtained as below

$$(w+10)(w+100) = (w+0.05503)w + 67.57k(w+7)$$

By solving the above equation for k , k is obtained as 1.62.

The corresponding controller TFs obtained are tabulated in Table 1.

The bode plot is shown in Figure 3(a) from which, phase margin is identified to be 86.4° at gain crossover frequency 110 rad/sec and gain margin is infinite. Hence, one can draw the conclusion that the designed controller provides robust compensation satisfactorily.

Table 1
Two DOF Controller Parameters for speed loop

	<i>w</i> -plane	<i>z</i> -plane
$C_{fs}(\cdot) = \frac{Q_s(\cdot)}{F_s(\cdot)}$	$0.148(w+100)/w$	$(0.148z - 0.1465)/(z - 1)$
$C_{bs}(\cdot) = \frac{H_s(\cdot)}{F_s(\cdot)}$	$(1.62(w+7))/w$	$1.62z - 1.619)/(z - 1)$

With respect to Table 1, the loop TFs for speed control loop is given by

$$TF_{loop} = \frac{H_s(w)B_s(w)}{F_s(w)A_s(w)} = \frac{1.62 \times (w+7) \times 67.57}{w(w+0.05503)}$$

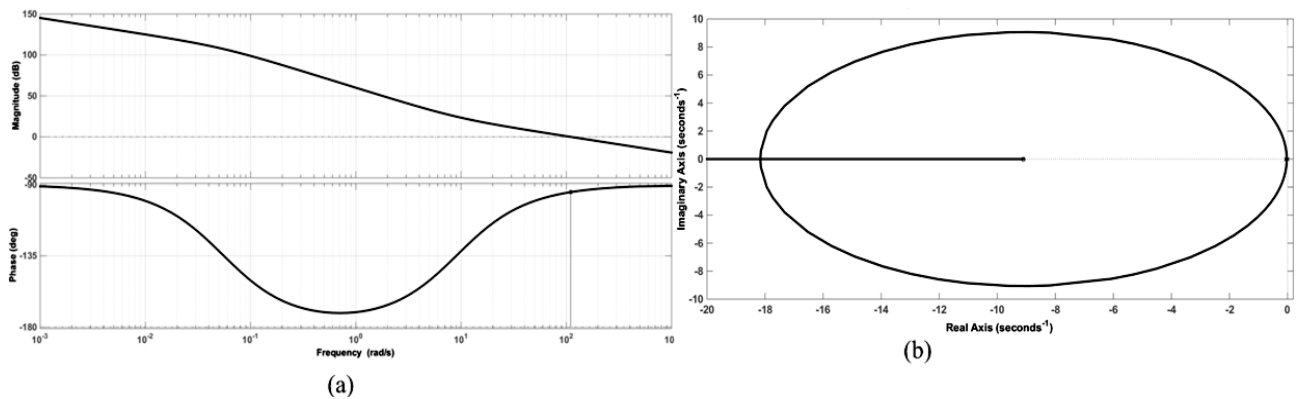


Figure 3: Speed loop (a) Bode plot and (b) Root locus plot

The root locus plot for speed loop TF is shown in Figure 3(b). From the observation of the root locus it can be stated that designed control system is unconditionally stable. Thus the system stability is preserved even if there is a variation in the open loop gain.

2. *Controller design for current loop:* Similar to the speed loop, the root locus plot of the inner loop plant will be the entire negative real axis of the *w*-plane beyond the open loop pole -20.55 . The desired closed loop pole location is chosen to be -200 so as to ensure 20 times lesser settling time. Thus the desired inner close loop TF becomes $\frac{147.167 \times 1.359}{(w+200)}$ with constant $\xi = 147.167$. Again, similar to the speed loop controller design, $F(w)$ polynomial, coefficients f_1 and f_0 are set to one and zero respectively. For current loop, $q(w)$ is chosen to be $\bar{q}(w) = w+100$. Now, the coefficients of $H(w)$ polynomial h_1 and h_0 are chosen to be 1 and 72, so that loop zero is placed at -72 . Gain k is obtained to be 220.8 by solving the following pole-placement equation.

$$(w+200)(w+100) = (w+20.55)w + 1.359k(w+72)$$

The controller TFs are obtained as in Table 2.

With respect to Table II, the loop TFs for current control loop is given by

$$TF_{loop} = \frac{H_c(w)B_c(w)}{F_c(w)A_c(w)} = \frac{220.8 \times (w+72) \times 1.359}{w(w+20.55)}$$

Table 2
Two DOF Controller Parameters for current loop

	<i>w</i> -plane	<i>z</i> -plane
$C_{fc}(.) = \frac{Q_c(.)}{F_c(.)}$	$147.167(w+100) / w$	$(147.167z - 145.7) / (z-1)$
$C_{bc}(.) = \frac{H_c(.)}{F_c(.)}$	$(220.8(w+72) / w$	$(220.8z - 219.2) / (z-1)$

From the bode plot depicted in Figure 4(a), phase margin is identified to be 80.7° at 308 rad/sec. The root locus plot of the current loop is shown in Figure 4(b). Just like the speed loop, current loop control system is also unconditionally stable i.e. change in open loop gain will not affect the stability of the inner loop. Alternately the gain margin is infinite.

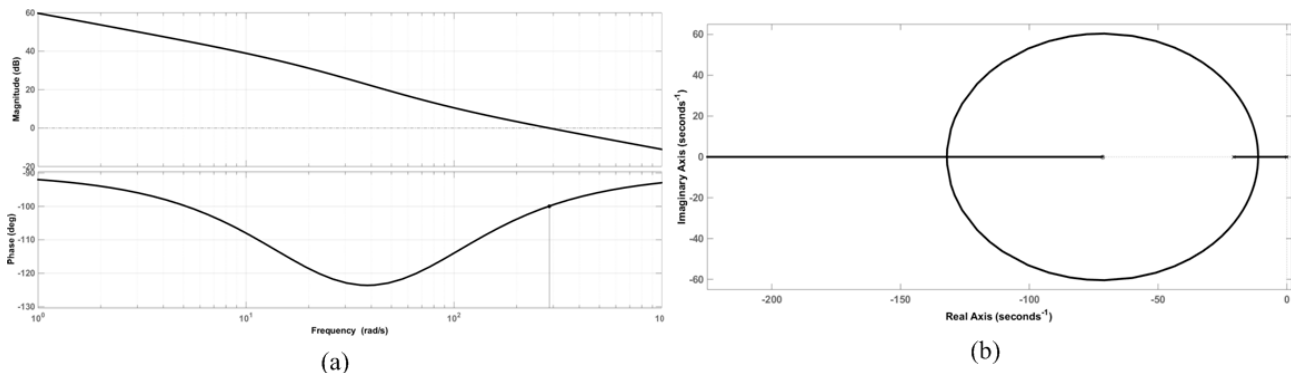


Figure 4: Current loop (a) Bode plot and (b) Root locus plot

5. PERFORMANCE COMPARISON OF DISCRETE TWO DOF WITH ONE DOF PI CONTROL

Two tests are carried out to proof the effectiveness of the proposed control scheme firstly reference speed tracking and secondly disturbance rejection. Also the results obtained are compared with that of discrete PI control. The parameters for the PI controllers are obtained to have similar bandwidth as in the case of two DOF control. This is done for to the comparison purpose only. The PI controller parameters are obtained as in Table 3.

Table 3
PI Controller Parameters

	<i>w</i> -plane	<i>z</i> -plane
Speed Loops	$(1.675w + 6.7) / w$	$(1.675z - 1.674) / (z-1)$
Current Loops	$(215w + 860) / w$	$(215z - 214.95) / (z-1)$

1. *Speed tracking*: For this test the IM is operated in 100 rad/sec, 50 rad/sec, 100 rad/sec and 150 rad/sec respectively with step changes at times 10 sec, 20 sec and 30 sec. A load torque of 20.37% is maintained throughout the entire period. The corresponding speed responses are shown in Figure 5(a), which depicts an overdamped response with a settling time of 0.7 sec for two DOF control and with PI control shows an underdamped response with overshoot around 10% and settling time 0.7 sec. The discrete PI control scheme speed response exhibits overshoot which is undesirable for many process industries, which can be overcome by the two DOF control scheme as it gives overdamped

response for same controller bandwidth or settling time. The reference flux is set at 0.75 Wb and the controller is maintaining it during the entire period. The flux response for change in speed reference is portrayed in Figure 5(b), which exhibits a settling time of around 0.7 sec.

2. *Disturbance rejection:* To examine this property, the IM is operated at constant speed 100 rad/sec. Initially the motor was loaded at 20.37%. The external load torque is then changed to respective levels at, 40.73%, 20.37% and 61% at time 10 sec, 20 sec and 30 sec. The corresponding speed response is shown in Figure 5(c). With both the control schemes speed settles down to its reference value within 0.7 sec. The flux responses are shown in Figure 5(d). Figure 5(e) shows the $d - q$ components of current changes during the load change. It is observed that the proposed control strategy is capable of disturbance rejection.

6. DISCRETE MRAS OBSERVER

The MRAS type observer is a well-established observer technique. The basic idea of MRAS is to compare the output rotor fluxes from the two reference and adaptive systems and correspondingly adapt the speed variable to be observed. In this work, a discrete time MRAS observer is modelled with respect to the discrete mathematical model in (1). The sampled version of the continuous time rotor and stator flux equation can be written as:

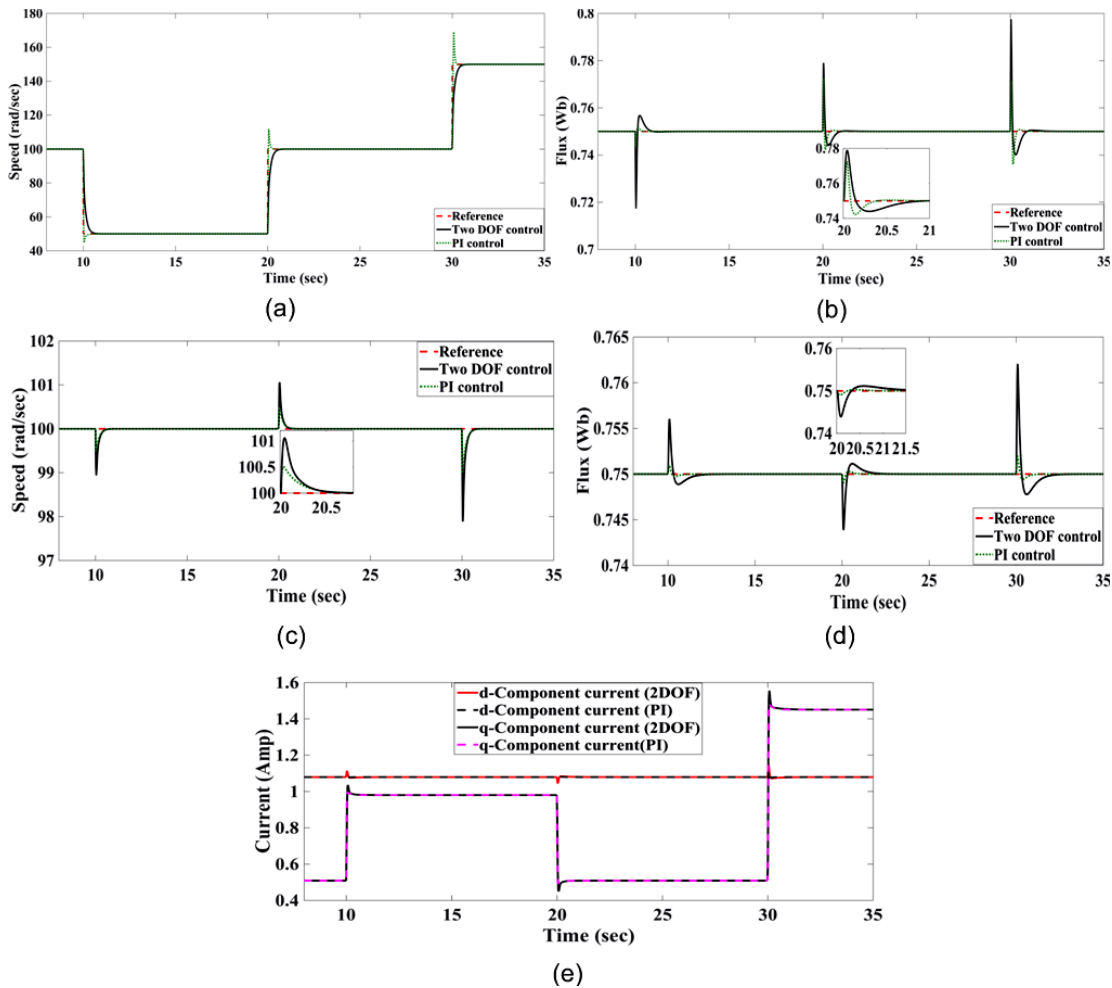


Figure 5: (a) Speed response to step change in reference speed (b) Flux response to step change in reference speed (c) Speed response to step change in Load torque (d) Flux response to step change in Load torque (e) d-q component stator current profile during load changes.

$$\begin{aligned}\phi_{\alpha\beta rk} &= L_r I_{\alpha\beta rk} + L_m I_{\alpha\beta sk} \\ \phi_{\alpha\beta sk} &= L_s I_{\alpha\beta sk} + L_m I_{\alpha\beta rk}\end{aligned}\tag{10}$$

From these equations the reference model for the discrete IM model can be obtained as

$$\phi_{\alpha\beta rk} = \frac{L_r}{L_m} \phi_{\alpha\beta sk} - \frac{L_r}{L_m} \sigma I_{\alpha\beta sk}\tag{11}$$

Again the rotor flux equation in (1), by removing trigonometric terms, neglecting the terms associated with higher order h , the following adaptive model is obtained

$$\begin{bmatrix} \hat{\phi}_{\alpha rk+1} \\ \hat{\phi}_{\beta rk+1} \end{bmatrix} = \alpha_d h p \begin{bmatrix} \frac{1}{hp} & -\hat{\omega}_k \\ \hat{\omega}_k & \frac{1}{hp} \end{bmatrix} \begin{bmatrix} \hat{\phi}_{\alpha rk} \\ \hat{\phi}_{\beta rk} \end{bmatrix} + L_m \alpha_d h \begin{bmatrix} I_{\alpha sk} \\ I_{\beta sk} \end{bmatrix}\tag{12}$$

Now for estimation of the speed $\hat{\omega}_k$ the following equation can be written [17]

$$\hat{\omega}_k = (\hat{\phi}_{\alpha rk} \phi_{\beta rk} - \phi_{\alpha rk} \hat{\phi}_{\beta rk}) \left(K_p + K_i \frac{h}{z-1} \right)\tag{13}$$

Therefore, considering (9) as reference model and (12) as adaptive model, speed can be observed to nullify error term in (13) with the help of the discrete PI type regulator.

7. PERFORMANCE OF DISCRETE MRAS OBSERVER

The effectiveness of the derived discrete time MRAS observer is examined for reference tracking and disturbance rejection with discrete time two DOF control strategy. The controller parameters are maintained at their same respective values as in case of without observer.

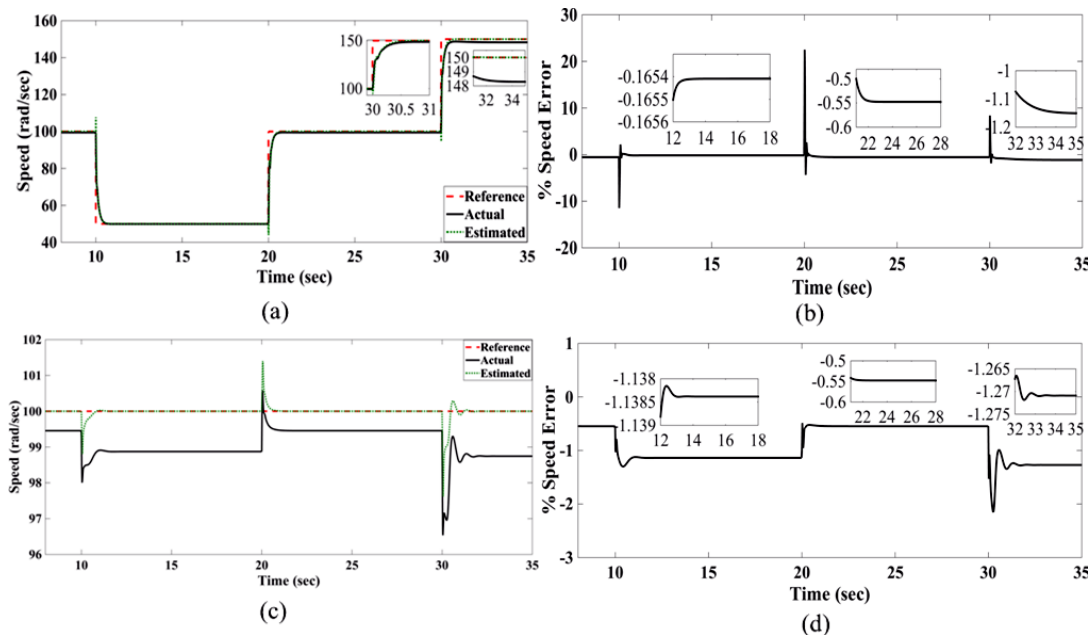


Figure 6: Speed response with observer feedback (a) During reference speed variation (b) % speed error during reference speed variation (c) During load torque variation (d) % speed error during load torque variation.

The same control topology is utilized as shown in Figure 2(a). Also the command reference speed for tracking test and the command load disturbance profiles are same as in case of without observer. The results obtained from discrete time MRAS observer are shown in Figure 6. The proportional and integral gains for the adaptive mechanism of MRAS observer in section VI are set at 200 and 800, respectively.

Figure 6(a) exhibits the comparative responses of MRAS observer and actual speed in case of reference tracking and corresponding % error is depicted in Figure 6(b), while the speed response and corresponding % error during the load disturbance rejection test are shown in Figure 6(c) and Figure 6(d) respectively. From the observation of the results following conclusions can be drawn.

- The derived discrete time MRAS observer is capable of estimating the speed with some acceptable error in the estimation.
- The maximum % error in speed tracking test is found to be -1.15% which is exhibited during 150 rad/sec speed reference.
- The maximum % error in load disturbance rejection test is found to be -1.27% which is exhibited during 61% load.

8. CONCLUSION

In this work, a synchronous frame discrete time model for induction motor is considered. A conventional continuous time field orientation like control strategy is developed in context with the two DOF controller for the derived IM dynamics. Two pairs of two DOF controllers are used to control speed, flux, d-axis component of stator current and q-axis component of stator current. The two DOF controllers are designed through root locus technique so as to achieve robust loop shaping and performance. The performance of the two DOF control strategy is compared with that of the PI controller designed with same bandwidth. The two DOF controllers are found to be fulfilling the pre-set robustness standards. Disturbance rejection capability of the proposed two DOF controllers is examined through load torque perturbation. From the performance point of view the two DOF control scheme exhibits better response without any overshoot in speed response compared to one DOF PI control. Further, the effectiveness of the derived discrete MRAS observer is tested by feeding the estimated speed to the two DOF control strategy. The discrete MRAS observer is found to be worked successfully even under load perturbation with allowable estimation error.

REFERENCES

- [1] Jorge Rivera Domínguez, "Discrete-Time Modeling and Control of Induction Motors by Means of Variational Integrators and Sliding Modes—Part I: Mathematical Modeling", *IEEE Transactions on Industrial Electronics*, Volume: 62, Issue: 9, pp: 5393 – 5401, Sep. 2015,
- [2] O. Elmaguiri and F. Giri, "Digital Back Stepping Control of Induction Motors," in *Proc. ISIE*, 2007, pp. 221–226.
- [3] F. Alonge, F. D'Ippolito, A. Fagiolini, and A. Sferlazza, "Extended Complex Kalman Filter for Sensor Less Control of an Induction Motor," *Controln Eng. Pract.*, Vol. 27, pp. 1–10, May. 2014.
- [4] R. Vieira, C. Gastaldini, R. Azzolin, and H. Gründling, "Discrete-Time Sliding Mode Speed Observer for Sensor Less Control of Induction Motor Drives," *IET Electr. Power App*, Vol. 6, No. 9, pp. 681–688, Nov. 2012.
- [5] Manoj Swargiary; Jayati Dey; Tapas Kumar Saha; Swagata Kumar Mohanty; Sankar Narayan Mahato "Two Degree of Freedom Control of IM Modeled Through Discrete Lagrangian Approach" *IEEE Tencon*, 2016, pp. 3498 - 3501.
- [6] Mituhiko Araki and Hidefumi Taguchi "Two-Degree-of-Freedom PID Controllers", *International Journal of Control, Automation, and Systems*, Vol. 1, pp. 401 – 411, Dec. 2003.

- [7] Jayati Dey and Tapas Kumar Saha “Design and Performance Analysis of Two Degree-of-freedom (2 DOF) Control of DC-DC Boost Converter”, *IEEE International Conference on Industrial Technology (ICIT)*, 2013, pp. 493 – 498.
- [8] Qun Zhu, Zhonggang, Yanqing Zhang, Jianbo Niu, Yan Li, and Yanru Zhong “Research on Two-Degree-of-Freedom Internal Model Control Strategy for Induction Motor Based on Immune Algorithm”, *IEEE Transactions on Industrial Electronics*, Vol. 63, pp. 1981-1992, Mar. 2016.
- [9] Tianchai Suksri, and Satean Tunyasirirut “T-DOF PI Controller Design for a Speed Control of Induction Motor”, *International Journal of Mechanical, Aerospace, Industrial, Mechatronic and Manufacturing Engineering*, Vol. 1, pp. 636-640. 2007,
- [10] I. M. Horowitz, *Synthesis of Feedback Systems*, Academic Press, 1963.
- [11] Gildes Bensancon, *Nonlinear Observers and Application*, Springer, 2007.
- [12] Francesco Alonge, Filippo D’Ippolito, Antonino Sferlazza, “Sensor Less Control of Induction-Motor Drive Based on Robust Kalman Filter and Adaptive Speed Estimation” *IEEE Transactions on Industrial Electronics*, Vol. 61, pp. 1444-1453, Mar. 2014.
- [13] Hassan K. Khalil, Elias G. Strangas, Sinisa Jurkovic “Speed Observer and Reduced Nonlinear Model for Sensor Less Control of Induction Motors”, *IEEE Transactions on Control Systems Technology*, Vol. 17, Issue: 2, pp. 327 – 339, Mar. 2009.
- [14] Angelo Accetta, Maurizio Cirrincione, Marcello Pucci “ Closed-Loop MRAS Speed Observer for Linear Induction Motor Drives” *IEEE Transactions on Industry Applications*, Vol. 51, pp. 2279 – 2290, May. 2015.
- [15] Ch. Naga Koti Kumar, S.Sundeeep, Ch.Durga Prasad, “Optimal Control of Induction Motor with Kalman Filter” *ICAESM, 2012*, pp. 39-45.
- [16] J. Cortés-Romero, A. Luviano-Juárez, and H. Sira-Ramírez, “A discretetime observer-based control for induction motors,” in *Proc. IECON*, 2010, pp. 17–22.
- [17] B. K Bose, *Modern Power Electronics and AC Drives*, PHI Learning Private Limited, 2002.
- [18] Paul Krause, Oleg Wasynczuk, Scott Sudhoff, Steven Pekarek, *Analysis of Electric Machinery and Drive Systems*, IEEE Press, 2013.